99-GT-409

EXPERIMENTAL INVESTIGATIONS OF STALL FLUTTER IN A TRANSONIC CASCADE

BREAK

Karsten Ellenberger and Heinz E. Gallus

Institut für Strahlantriebe und Turboarbeitsmaschinen
RWTH Aachen, University of Technology
Templergraben 55, D-52062 Aachen, Germany

ABSTRACT

The design of modern gas turbines is more and more based on flow simulations by numerical calculation models. Due to the different influence parameters the development and verification of these codes requires detailed data bases, which can only be provided by experimental investigations. The demand of increasing power density leads to higher Mach Numbers up to transonic ranges. Due to the thin blade profiles the risk of stall flutter becomes an extraordinary point of interest. Therefore, in a transonic wind tunnel a cascade of nine compressor blades designed by MTU Munich were investigated at different inlet Mach numbers and incidence angles. To get information about flow behavior at steady state, profile pressure distribution was measured at midspan with pressure taps on profile surface. In order to provide information about the overall flow field oil flow visualization and Schlieren technique were applied for the investigation at steady state. For flutter simulation the blade in the middle position of the cascade was forced to torsional oscillating movement by an electromagnetic shaker system with a frequency of $f = 310.0$ Hz. The flow behavior with oscillating and fixed center blade was investigated at midspan by means of dynamic pressure transducers and hot films glued on profile probes. The results of these investigations are presented in this paper especially up to the appearance of stall flutter.

NOMENCLATURE

c	chord length of blade = 41.19 mm
A	area of cross section of wind tunnel
t_b	pitch length of blade = 25.67 mm
x	coordinate in axial chord direction
t	time
i	incidence angle
f	flutter frequency = 310.0 Hz

v	velocity
Ma	Mach number
$\dot{m}$	mass flow rate
ω^*	reduced frequency = $(2 \pi f c) / v_{is, ref}$
Re	Reynolds number = $(\rho_{is, ref} v_{is, ref} c) / \mu_{ref}$
T	temperature
p	pressure
$c_{p, s}$	static pressure coefficient = $(p_s - p_{s, ref}) / (p_t - p_{s, ref})$
$c_{p, d}$	dynamic pressure coefficient = $|p_{fft}| / [(|\alpha_{max}| / 1°)(p_t - p_{s, ref})]$
SS, PS	suction side, pressure side of blade
U, U_0	voltage , zero-flow voltage
REF	reference measurement position of static pressure for operating point calculation (Fig. 1)

Greek Symbols

$\Delta\beta$	blade turning angle = 13.0°
λ	stagger angle = 49.5°
α	amplitude angle of oscillating blade
ρ	density of air
μ	dynamic viscosity of air
ϕ	phase shift at flutter frequency

Subscripts

s, d, t	static value, dynamic value, total value
is	isentropic value
fft	FFT-amplitude at flutter frequency
ref	operating point reference value
ea	ensemble averaged value
rms	root mean squared value

INTRODUCTION

The flow around the profile with transonic inlet Mach numbers causes shock boundary layer interactions with high profile losses. To reduce losses thin blade profiles are designed. Due to this blade geometry, the risk of blade fractures becomes more and more important. Especially self-excited oscillation could be induced by flow separations on the profile surface. These separation regions are caused by different incidence angles. Therefore, the effects of blade vibrations must be considered during the design of modern blade geometry. The development of modern blade profiles is more and more based on numerical calculation codes. For verification and calibration of these flow simulation models, detailed knowledge about flow phenomena like blade vibrations, shock boundary layer interactions and their effects must be available. This knowledge has to be provided by experimental investigations like the one presented in this paper.

Two different oscillating mechanisms of blade movement can be found in turbomachines, the bending oscillation mode and the torsional oscillation mode. Detailed information about the different travelling modes of blade vibration can be found at Meher-Homji [1]. Furthermore, some authors concentrated their investigations especially on the torsional flutter mechanism. Hennings [2], for example, had examined experimental self-excited and forced oscillation in a low speed linear cascade. Schaber et al. [3] investigated coupled blade bending and torsional shaft vibrations in turbomachines and Frischbier et al. [4] published on blade vibrations of a high speed compressor blisk-rotor. Numerical flow simulations of blade vibrations were carried through by Weber et al. [5] as well as parametric studies of the flutter stability of turbomachine cascades by Försching [6]. However, for the validation of numerical codes and their improvement comparisons of calculated values with experimental data are necessary. Therefore, the aim of this research is the physical interpretation of experimental data as well as the achievement of

detailed data bases for the development and calibration of numerical codes.

EXPERIMENTAL FACILITY AND INSTRUMENTATION

To provide an experimental data base a blade row of nine compressor blade profiles designed by MTU Munich was investigated in a transonic wind tunnel at different Mach numbers and incidence angles. Furthermore, to provide knowledge about physical flow phenomena at stall flutter the blade in middle position of the cascade was forced to torsional oscillating movement by an electromagnetic shaker system with a frequency of $f = 310.0$ Hz. Steady and unsteady measurement techniques were applied at different positions in the blade row, with oscillating and fixed middle blade, to get detailed information about flow behavior at inlet and outlet section of the cascade as well as on profile surface. The results of these investigations are presented in this paper up to the appearance of stall flutter.

Test Facility

The experimental investigations were carried out in a transonic wind tunnel with continuously variable incidence angles up to stall on the profile surface. The cross section area at cascade inlet is $A = 116.0$ mm height x 79.0 mm width. The chord length of the compressor blades designed is $c = 41.192$ mm with a stagger angle of $\lambda = 49.5°$ and a turning angle of $\Delta\beta = 13.0°$. The blade pitch is $t_b = 25.67$ mm. Detailed information about the arrangement of the cascade and the implementation of the several regulation systems are presented in Fig.1. For variation of incidence angle the blade row was connected with a turnable sidewall. To minimize boundary layer development at the inlet of the test rig two by-pass systems were integrated in the sidewalls in front of the blade row. In all examined operating points
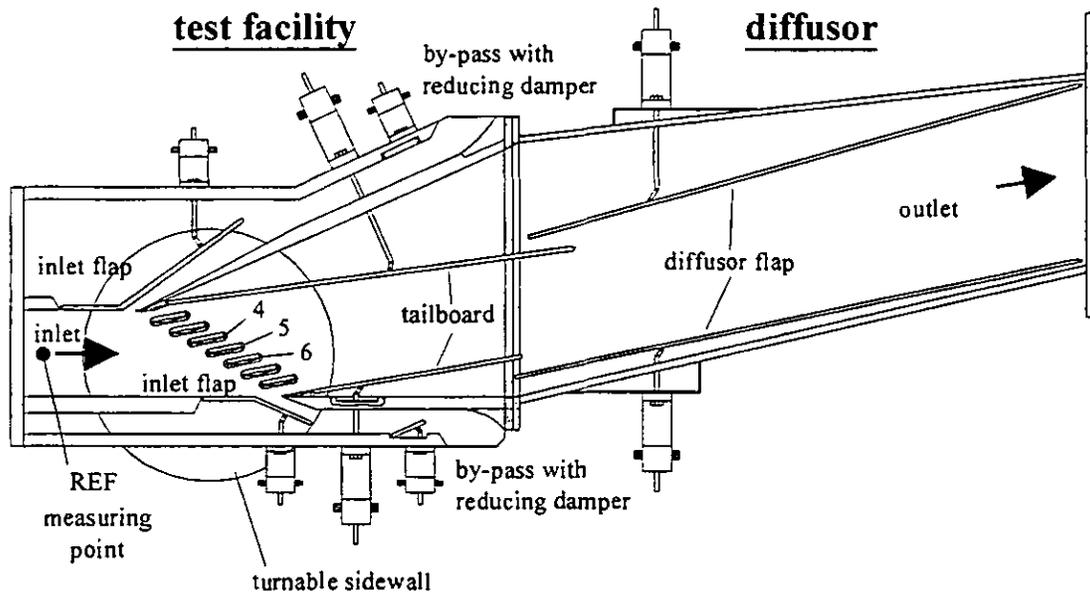
Fig.1 : Cross Section View of the Test Facility and the Variable Diffuser

periodic flow conditions up- and downstream the cascade could be achieved by several flap systems controlled with a number of sidewall pressure taps. These measuring points were arranged parallel to the leading and trailing edge of the blades. Upstream of the test facility total temperature and total pressure was detected in a settling chamber. Furthermore, for calculation of isentropic inlet Mach numbers local static pressure was measured at reference position (point < REF > in Fig.1. For variation of inlet Mach number the mass flow rate could be controlled with a throttle in the pipeline downstream of the test facility.

For the simulation of blade vibration the blade in the middle position of the cascade was forced to torsional oscillation by electromagnetic shakers. This shaker system was mounted fixed to the turnable sidewalls of the test facility. Thus, blade vibrations were forced with a frequency of $f = 310.0$ Hz and an maximum amplitude angle of $\alpha = \pm 0.65°$ was achieved. This amplitude was recorded with two acceleration transducers fastened at the torsion bar. The center of rotation of the oscillating blade was at about 53% chord length.

To minimize losses the diffuser downstream of the cascade was designed with variable sidewalls.

Measuring System

The flow behavior, with oscillating and fixed center blade, was investigated with a number of different measurement techniques on profile surface. Therefore, these measurement blades were mounted in the center position of the cascade as well as at the neighboring positions with fixed and oscillating middle blade. The various profile probes are presented in Fig.2.
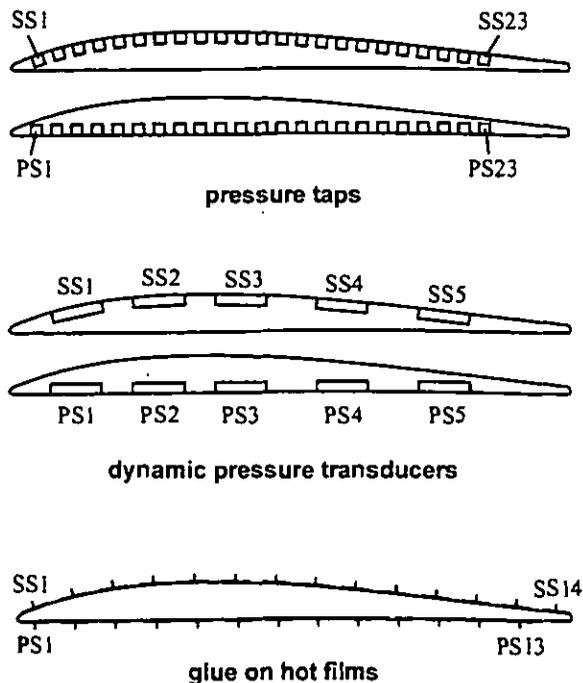
SS1   SS23

PS1   PS23

pressure taps

SS1   SS2   SS3   SS4   SS5

PS1   PS2   PS3   PS4   PS5

dynamic pressure transducers

SS1   SS14

PS1   PS13

glue on hot films

Fig.2 : Steady and Unsteady Measurement Techniques on Suction and Pressure Side of Profile Surface

To get information about steady state flow behavior with fixed center blade, profile pressure distributions were measured at midspan with pressure taps on the profile surface. Furthermore, local static pressure was detected with a number of pressure taps arranged in the sidewall parallel to leading and trailing edge of the blade profiles. To provide knowledge about the overall flow field, oil flow visualization and Schlieren techniques were applied for the examination at steady state in the middle position of the blade row.

The unsteady flow behavior was investigated with two different measurement techniques. The pressure fluctuation was measured with dynamic pressure transducers (Kulite LQ-47-25) at midspan of the oscillating middle blade, as well as at their neighboring positions in the cascade. Information about the boundary layer behavior on blade profile of fixed and oscillating center blade, as well as the influence of torsional blade movement at the neighboring positions of the blade row could be achieved with a number of hot film probes (Dantec) glued on the blade surface at midspan.

Due to the thin blade profiles pressure taps and dynamic pressure transducers on suction side and pressure side had to be arranged in two different blades. The glue on hot film probes could be arranged at midspan of one blade profile. To reach high resolutions 23 pressure taps as well as 5 dynamic pressure transducers were used on each side of the blade. The information about boundary layer behavior was detected with 14 hot film sensors on suction side and 13 hot film sensors on pressure side.

Operating Points

To provide detailed data of flow behavior of a compressor cascade at transonic velocities up to the appearance of stall with oscillating ($f = 310.0$ Hz ; $\alpha = \pm 0.65°$) and fixed center blade experimental investigations were executed at different operating points. The inlet Mach number, calculated with the static pressure measured at the reference position REF (Fig.1), was varied step by step between $Ma_{is, ref} = 0.60$ and $Ma_{is, ref} = 0.88$ by regulation of mass flow rate. At the highest inlet Mach number a mass flow rate of $m_{is} = 3.6$ kg/s was measured. For the simulation of different inlet flow angles at leading edge of blade profile incidence angles from $i = -2.5°$ (negative incidence) up to $i = 5.0°$ (positive incidence) were realized at each Mach number. In the range of described inlet Mach numbers Reynold numbers between $Re = 5.5 \times 10^{+5}$ and $Re = 8.0 \times 10^{+5}$ were realized.
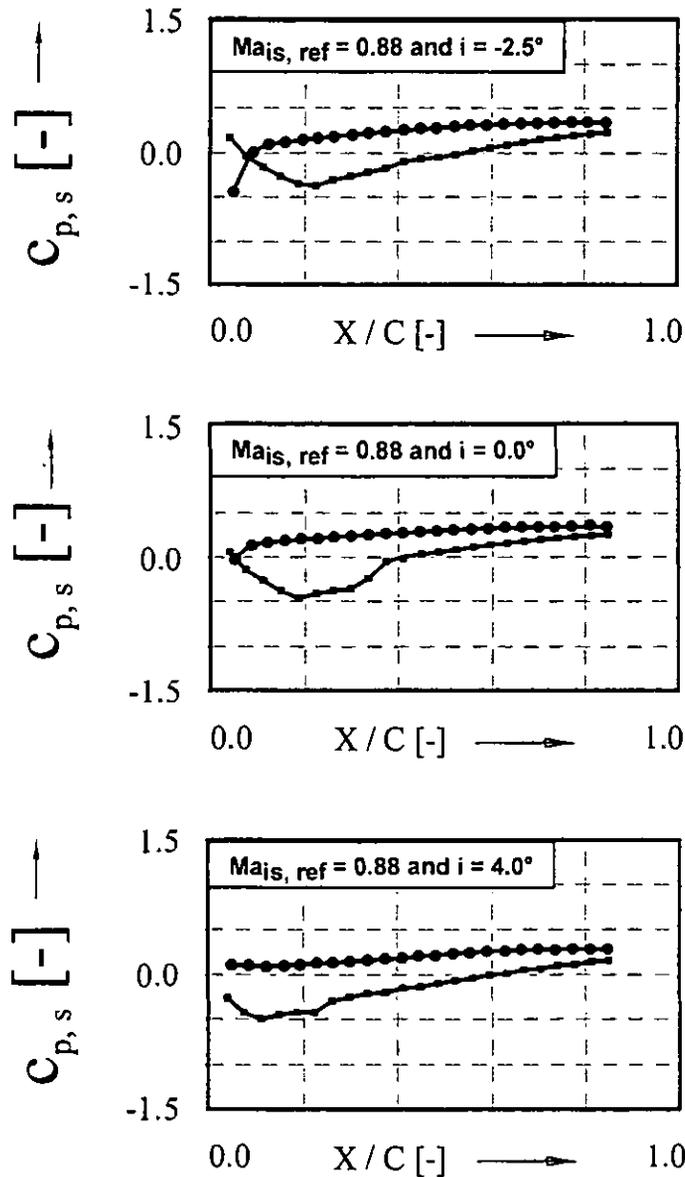
RESULTS AND DISCUSSION

For the investigations of blade vibrations at transonic inlet Mach numbers different measurement techniques were applied. To present the experimental data in an obvious form, the analyses and discussions are subdivided in chapters of measurement techniques, which were used. The results of these experiments will be presented in this paper for several incidence angles at the inlet Mach number of $Ma_{is, ref} = 0.88$.

Steady Pressure Distribution

To get basic information about flow behavior on profile surface at steady state profile pressure distributions were measured at

3

midspan. The results of these measurements without an oscillating blade are presented in Fig.3 for different incidence angles.. At these operating points the suction side pressure taps were positioned at the middle blade of the cascade (blade 5) and the pressure side taps at the neighboring blade below (blade 6). For better understanding of the blade nomenclature see Fig.1.
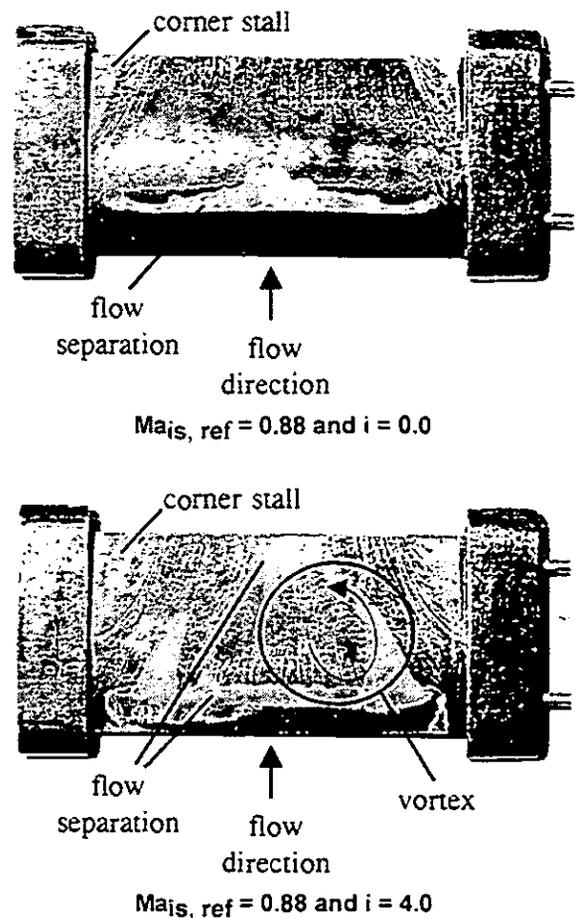
at 12% chord length. At the negative incidence angle of $i = -2.5°$ no flow separation caused by the shock boundary layer interaction could be recorded on blade profile surface with pressure taps. For detailed analyses of flow separation development, further measurement techniques had to be used like oil flow visualization and Schlieren technique.
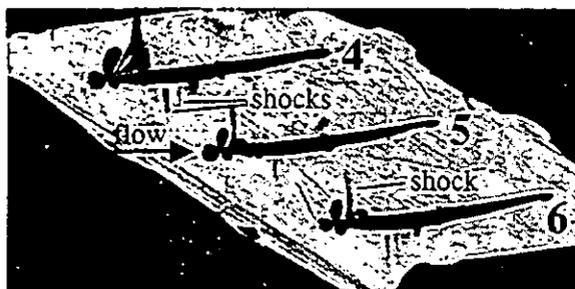
Flow Visualization

To enlarge knowledge about flow behavior oil flow visualization was applied at steady state on the profile surface of the middle blade. Therefore, a mixture of oil and Titan-IV-oxide was distributed on a black painted profile surface. The wall shear stresses cause a transport of this mixture. The intensity of transport is dependent on different flow velocities along the surface. Especially, with this measurement technique the appearance and development of flow separation, corner stall and vortices around the profile could be detected. Furthermore, physical phenomena of profile pressure distributions detected with static pressure taps at several operating points could be confirmed. Examples of the oil flow visualizations are shown in Fig.4 for different incidence angles.
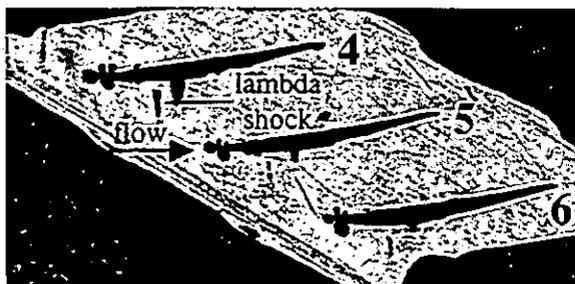

$Ma_{is, ref} = 0.88$ and $i = 0.0$

Fig.3 : Static Pressure Distribution Suction Side Blade 5, Pressure Side Blade 6

Due to the shock system, flow separation inside the boundary layer could be recorded at 20% chord length on suction side of profile surface for zero degree incidence. The static pressure coefficient minimum or, respectively, the Mach number maximum is shifted upstream after increasing positive incidence angles. At the incidence angle of $i = 4.0°$ the pressure plateau on suction side could be detected

$Ma_{is, ref} = 0.88$ and $i = 4.0$

Fig.4 : Oil Flow Visualization on Profile Surface Suction Side Blade 5

4

Flow separation at midspan induced by a shock system was detected at the first 20% of chord length on profile suction side at the incidence angle of i = 0.0° as well as i = 4.0°. The movement of separation, due to the movement of the shock system upstream to the profile leading edge caused by increasing incidence angles is also shown in this figure. Beside the flow information already found with pressure taps, more and more three dimensional influences forced by higher positive flow angles could be stated. As shown in Fig.4 for the positive incidence angle of i = 4.0° two symmetric vortices were detected on the profile suction side. These vortices were caused by a pressure gradient inside the boundary layer on profile surface normal to flow direction. The pressure gradient resulted from the difference between sidewall pressure levels (no shock in the wall boundary layer) and midspan after the shock system, ref. [7]. Furthermore, a boundary layer separation at about 60% chord length at midspan was also detected at the same operating point.
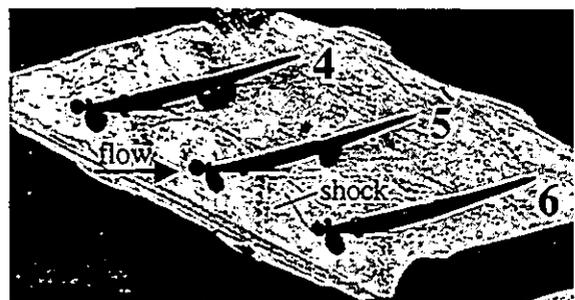
Another flow visualization technique is the Schlieren technique based on the visualization of density gradients (Fig.5).

Ma$_{is, ref}$ = 0.88 and i = -2.5°

Ma$_{is, ref}$ = 0.88 and i = 0.0°

Ma$_{is, ref}$ = 0.88 and i = 4.0°

Fig.5 : Flow Visualization with Schlieren Technique Blade 4 (Upper), 5 (Middle) and 6 (Lower Blade)

Three blade profiles in the middle position of the cascade, connected with a changeable part of sidewalls manufactured in Plexiglas, were investigated at steady state and photographed with a reflex camera. The axis of optical light was arranged in a z-formation.

At the incidence angle of i = -2.5° two shocks were detected between 25% and 35% of chord length on suction side (further shaded zones were due to blade mounting in the Plexiglas wall). Furthermore, another shock at pressure side leading edge was visible at the same operating point. Due to the extremely accelerated flow the shock extended forward the neighboring profile suction side between 40% and 45% of chord length. At the incidence angles of i = 0.0° and i = 4.0° the shock position at blade suction sides was moving upstream, the shock strength was increasing and the width was growing obviously due to shock oscillation with increasing incidence angle.

Unsteady Pressure Distribution

The influence of blade vibrations on the flow around the profile was investigated at frequencies of f = 310.0 Hz with high resolution dynamic pressure transducers (Kulite LQ-47-25) mounted flush with the profile surface. These transducers were insensitive to acceleration, so a correction of pressure values was not necessary.

Dynamic pressure fluctuations caused by shock oscillation were detected on profile surface of the vibrating blade as well as the influence of torsional movement on the neighboring blades. To get detailed information about blade loading at the different operating points, all results will be graphical plotted with dynamic pressure coefficient and phase shift, calculated with fast Fourier transformation, ref. [8]. Furthermore, a negative phase shift is synonymous for a pressure signal following the torsional movement of the oscillating blade.

At the incidence angle of i = -2.5° (Fig.6), the shock movement at pressure side leading edge detected with transducer PS1 (12% chord length) on the oscillating blade 5 caused a dynamic pressure coefficient amplitude of nearly c$_{p, d}$ = 0.511 (p$_d$ = 18000 Pa).

suction side blade 4   pressure side blade 5
(blade 5 oscillating)   (oscillating)
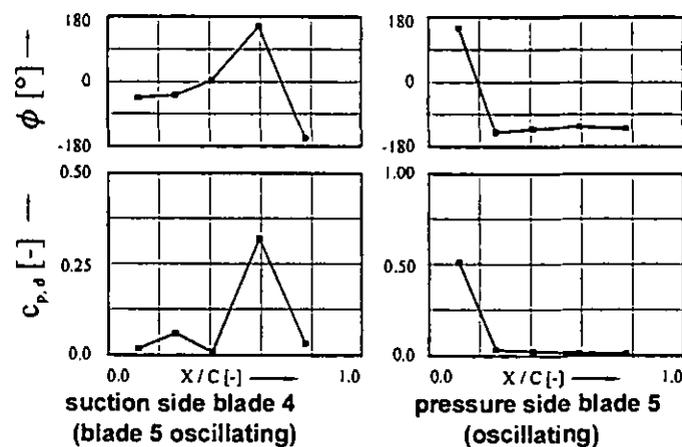
Fig.6 : Dynamic Pressure Coefficient and Phase Shift
Ma$_{is, ref}$ = 0.88 and i = -2.5° ; ω^* = 0.276

Another pressure fluctuation with an amplitude of c$_{p, d}$ = 0.319 (p$_d$ = 12000 Pa) induced by the same shock wave (there is no phase shift

5

between these two signals) was measured on suction side of the upper neighboring blade 4 at 59% chord length (position SS4). Due to the blade position of transducer SS2 at 27% chord length, another dynamic pressure coefficient maximum with an amplitude of $c_{p, d}$ = 0.059 induced by the shock system on suction side, shown in Fig.5, could also be detected. In contrast to the pressure fluctuation on SS4 induced by the shock oscillation on the torsional vibrating blade itself, that amplitude caused by the shock movement on the fixed blade 4, measured with transducer SS2, is an example for the influence of blade vibrations onto their neighboring blades. This signal is following the blade movement within a short time delay.

Since shocks at pressure side occurred only for negative incidence, in the following only signals along the suction side will be considered. At the inlet Mach number $Ma_{is, ref}$ = 0.88 and the incidence angle i = 0.0°, as designed, pressure fluctuations caused by blade vibrations were measured at position SS1 (12% chord length) and SS2 (27% chord length) shown in Fig.7.
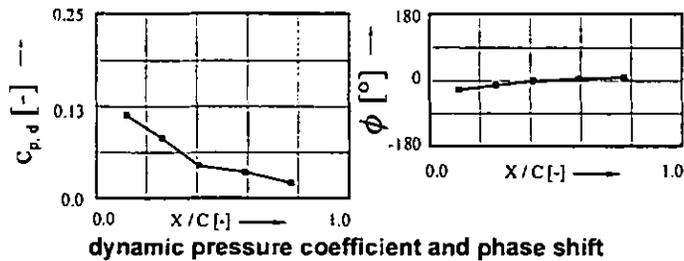

dynamic pressure coefficient and phase shift

**Fig.7 : Dynamic Pressure Coefficient and Phase Shift
Suction Side Blade 5 (Oscillating)
$Ma_{is, ref}$ = 0.88 and i = 0.0° ; ω^* = 0.279**

Especially at the measuring point SS1 a dynamic pressure coefficient amplitude of $c_{p, d}$ = 0.113 (p_d = 5000 Pa) with nearly the same phase relation as torsional oscillation induced by shock movement was recorded. This fluctuation was induced by the oscillation of the lambda shock shown in Fig.5. Downstream of position SS1 the values of pressure fluctuations were decreasing. In Fig.8 the dynamic pressure distribution at midspan is shown for the same inlet Mach number and an increased incidence angle of i = 4.0°.
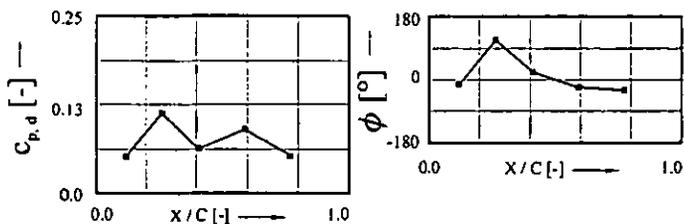

**Fig.8 : Dynamic Pressure Coefficient and Phase Shift
Suction Side Blade 5 (Oscillating)
$Ma_{is, ref}$ = 0.88 and i = 4.0° ; $\omega^°$ = 0.278**

In contrast to the incidence angle i = 0.0° with a decreasing signal along chord length two amplitude maxima could be detected at this operating point. The first maximum with an amplitude of $c_{p, d}$ =

0.112 (p_d = 4000 Pa) was measured at 27% chord length (position SS2) and the second one with an amplitude of $c_{p, d}$ = 0.090 (p_d = 3000 Pa) at 59% chord length (position SS4). As the first maximum with positive phase shift was induced by the oscillating shock system, the one at position SS4 with negative phase shift seemed to be caused by the fluctuation of the boundary layer separation. Fig. 4 supports this explanation by the onset of separation at about 60% chord length at midspan.

Unsteady Boundary Layer Behavior

For investigations on the development of boundary layer and turbulence behavior along profile surface, glue on hot film sensors were used at midspan for all operating points. Some of the hot film sensors near the pressure side leading edge were destroyed after a few operating points by little particles in the air flow. Therefore, only hot film signals on suction side with fixed and oscillating blade 5 will be presented at inlet Mach number $Ma_{is, ref}$ = 0.88. To compare the results each signal had to be made non-dimensional by use of zero-flow voltage, ref. [9]. For detailed interpretation of the hot film signals, the integral stochastic fluctuation coefficient was calculated with root mean square values, ref. [10]. Further information about hot film analyses is described in ref. [11] and ref. [12].

The boundary layer development along the profile surface on the fixed as well as oscillating blade 5 at the highest Mach number and the incidence angle i = -2.5° the integral stochastic fluctuations are plotted in Fig.9.

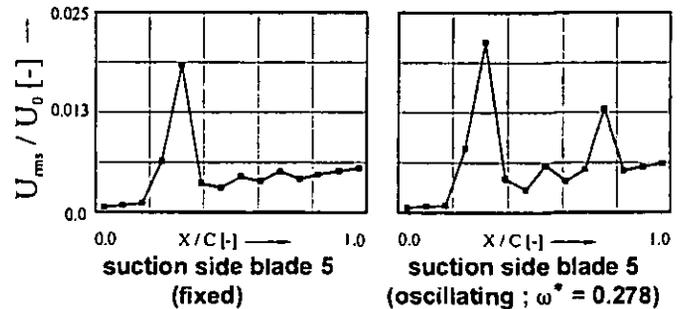suction side blade 5
(fixed)

suction side blade 5
(oscillating ; ω^* = 0.278)

**Fig.9 : Integral Stochastic Fluctuation Coefficient
$Ma_{is, ref}$ = 0.88 and i = -2.5°**

The laminar-turbulent boundary layer transition could be clearly detected at a chord length of 20% on the fixed as well as vibrating blade 5. After the transition zone turbulence is decreasing on the fixed blade 5. On the oscillating blade 5 a second maximum of the integral stochastic fluctuation coefficient could be found at 75% chord length which was also detected at other incidence angles. The explanation for the appearance of the second very strong maximum could be given by separation of the turbulent flow due to former experiences. On the other hand, the single peak measured only by sensor SS11 could be caused by a damaged hot film sensor, since both adjacent sensors showed only very low and equal levels, and, additionally, the other measurement techniques give no evidence for turbulent separation. At i = 0.0° incidence and isentropic inlet Mach number $Ma_{is, ref}$ = 0.88 a transition zone was also detected at measurement positions SS4 and

6

SS5 on the fixed as well as oscillating blade 5 (Fig.10). In contrast to root mean square values at i = -2.5° incidence, the beginning of increasing turbulence on the oscillating blade 5 was observed closer to leading edge. Furthermore, this maximum is at the same position the flow separation was detected with static pressure taps as well as oil flow visualization. Due to the blade movement, there is only a small fluctuation of the turbulence maximum at 20% chord length, but a strong increase of the turbulent intensity within the separation region.
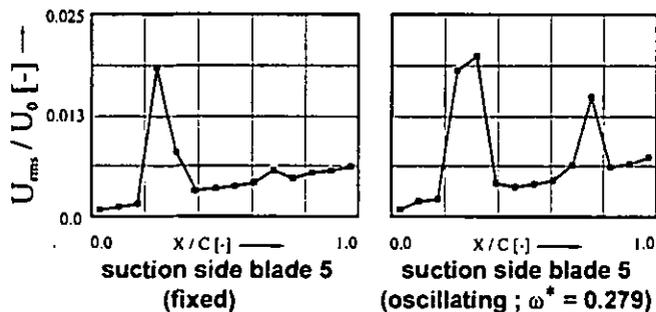
Fig.10 : Integral Stochastic Fluctuation Coefficient
$Ma_{is, ref} = 0.88$ and $i = 0.0°$

The measurements for an incidence angle of i = 4.0° were also performed at the highest inlet Mach number $Ma_{is, ref} = 0.88$.
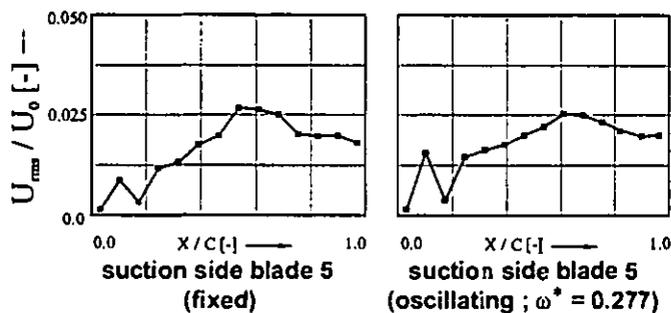

Fig.11 : Integral Stochastic Fluctuation Coefficient
$Ma_{is, ref} = 0.88$ and $i = 4.0°$

Fig. 11 revealed a flow separation after 30% chord length on the fixed as well as oscillating blade 5. Furthermore, the transition zone was shifted upstream with increasing incidence angles. Due to the second very strong turbulence level after 60% chord length on the fixed as well as oscillating blade 5, the boundary layer separation at about 60% chord length at midspan could also be detected with the glue on hot film sensors. Finally, all measured results confirmed the much higher turbulence intensity along the oscillating blade surface (blade 5). The second maximum in the stochastic distribution which could be found for i = -2.5° as well as i = 0.0° incidence at 75% chord length on the oscillating blade 5 was not measured at the incidence angle i = 4.0°.

CONCLUSIONS

Blade flutter is of main interest in modem compressor design. Especially, knowledge about flow behavior and boundary layer development along the profile surface needs detailed experimental investigation. With this data bases verification and calibration of numerical codes can be performed.

In a first step, the static pressure field upstream and downstream the cascade as well as on the blade surfaces was measured at steady state in order to control the periodicity of the flow. Furthermore, using Schlieren technique, oil flow visualization and pressure measurements the shock systems and flow separation along the profile surface were detected.

Due to increasing incidence angles, the movement of separation induced by the movement of the shock system upstream to the profile leading edge was measured with pressure taps. Furthermore, three dimensional influences forced by higher positive flow angles could also be stated with the help of oil flow visualization. At the isentropic inlet Mach number $Ma_{is, ref} = 0.88$ and the incidence angle i = 4.0°, for example, two symmetric vortices were detected on the blade suction side.

Information about the shock behavior on the torsionally oscillating blade 5 (f = 310 Hz) could be provided with dynamic pressure transducers. Especially at the highest isentropic inlet Mach number $Ma_{is, ref} = 0.88$ and the incidence angle i = -2.5° pressure fluctuations forced by blade oscillation were measured on the oscillating blade 5, as well as the induced effects on their fixed neighboring blades.

Boundary layer investigations using hot film sensors along suction and pressure side in the profile surface reveal that, due to the torsional movement, there was a small fluctuation of the transition point as well as a strong increase of the turbulence intensity within the separation region for the oscillating blade 5 compared with the fixed blade 5.

Furthermore, a second maximum of turbulence intensity was measured on the oscillating blade 5 near trailing edge (75% chord length) for the incidence angles of i = 0.0° and i = -2.5°. It is very likely, that this second increase is no indication of turbulent separation, but is caused by a defect sensor at this measurement position, since the adjacent sensors measured a very low turbulence level, and, additionally, the other measurement techniques give no evidence for turbulent separation.

Based on these experimental data, the development and verification of a numerical code was achieved. The results of these calculations will be presented by Brouillet et al. [13].

REFERENCES
[1] Meher-Homji, C.B., 1995, „Blading Vibration And Failures In Gas Turbines", part a up to part d, ASME 95-GT-418 up to -421

[2] Hennings, H., Send, W., 1996, „Experimental Investigation And Theoretical Prediction Of Flutter Behavior Of A Plane Cascade In Low-Speed Flow", ASME 96-GT-417

[3] Schaber, U., Mayer, J.F., Stetter, H., 1993, „Coupled Blade Bending And Torsional Shaft Vibration In Turbomachinery", ASME 93-GT-267

[4] Frischbier, J., Schulze, G., Zielinski, M., Ziller, G., Blaha, C., Hennecke, D.K., 1996, „Blade Vibrations Of A High Speed Compressor Blisk-Rotor - Numerical Resonance Tuning And Optical Measurements -", ASME 96-GT-24

[5] Weber, S., Benetschik, H., Peitsch, D., Gallus, H.E., 1997, „A Numerical Approach To Unstalled And Stalled Flutter Phenomena In Turbomachinery Cascades", ASME 97-GT-102

[6] Försching, H., 1996, „A Parametric Study Of The Flutter Stability Characteristics Of Turbomachine Cascades", ASME 96-GT-260

[7] Lösch-Schloms, R., 1995, „Experimentelle Untersuchungen zur Optimierung eines invers ausgelegten Verdichterprofilschnitts in einem ebenen Windkanal", Diss. RWTH Aachen

[8] Fransson, T.H., 1983, „Two Dimensional And Quasi Three Dimensional Experimental Standard Configurations For Aeroelastic Investigation In Turbomachine Cascades", Ecole Polytechnique Federale de Lausanne

[9] Halstead, D.E., Wisler, D.C., Okiishi, T.H., Walker, G.J., Hodson, H.P., Shin, H.-W., 1995, „Boundary Layer Development In Axial Compressors And Turbines", part I up to part 4, ASME 95-GT-461 up to -464

[10] Pieper, S.J., 1995, „Erfassung instationärer Strömungsvorgänge in einem hochtourigen, invers ausgelegten einstufigen Axialverdichter mit Vorleitrad", Diss. RWTH Aachen

[11] Oldfield, M.L.G., Kiock, R., Holmes, A.T., Graham, C.G., 1981, „Boundary Layer Studies On Highly Loaded Cascades Using Heated Thin Films And A Traversing Probe", Journal of Engineering for Power, Vol. 103

[12] Schulz, H.D., 1989, „Experimentelle Untersuchung der dreidimensionalen abgelösten Strömung in einem Axialverdichterringgitter", Diss. RWTH Aachen

[13] Brouillet, B., Benetschik, H., Volmar, Th., Niehuis, R. „Three Dimensional Navier-Stokes Computation Of A Flutter Cascade Near Stall Conditions", to be published at the International Gas Turbine Conference, Kobe, Japan, 1999